Single-photon frequency conversion via cascaded quadratic nonlinear processes

Tong Xiang, Qi-Chao Sun, Yuanhua Li, Yuanlin Zheng,[*] and Xianfeng Chen[†]

State Key Laboratory of Advanced Optical Communication Systems and Networks, School of Physics and Astronomy,
Shanghai Jiao Tong University, Shanghai 200240, China
and Key Laboratory for Laser Plasma (Ministry of Education), Collaborative Innovation Center of IFSA,
Shanghai Jiao Tong University, Shanghai 200240, China

Frequency conversion of single photons is an important technology for quantum interface and quantum communication networks. Here, single-photon frequency conversion in the telecommunication band is experimentally demonstrated via cascaded quadratic nonlinear processes. Using cascaded quasi-phase-matched sum and difference frequency generation in a periodically poled lithium niobate waveguide, the signal photon of a photon pair from spontaneous down-conversion is precisely shifted to identically match its counterpart, i.e., the idler photon, in frequency to manifest a clear nonclassical dip in the Hong-Ou-Mandel interference. Moreover, quantum entanglement between the photon pair is maintained after the frequency conversion, as is proved in time-energy entanglement measurement. The scheme is used to switch single photons between dense wavelength-division multiplexing channels, which holds great promise in applications in realistic quantum networks.

I. INTRODUCTION

Quantum networks rely on many nodes for quantum information storage and processing and optical channels connecting them [1]. To date, quantum storage and information processing have been demonstrated in a wide variety of physical systems, such as single atoms [2], atomic ensembles [3], rare-earth ions in solids [4], quantum dots [5], nitrogen-vacancy centers [6], and superconducting circuits [7]. They operate at different optical frequencies, thus single photons have to be converted to the telecommunication band before transfer in fiber for long distance quantum communication [8]. Moreover, dense wavelength-division multiplexing (DWDM) channels in fiber have been exploited in quantum communication to reduce the cost [9] and increase communication efficiency [10–12]. Optical cross-connect switching for single photons will become significantly important in the future. However, frequency mismatch between quantum systems and the DWDM channels would make it difficult to realize efficient quantum networks. To overcome this problem, it is crucial to realize tunable quantum frequency convertors while maintaining the quantum characteristics carried by photons.

For this purpose, sum frequency generation (SFG) and difference frequency generation (DFG) have been used to transfer the frequency of photons while preserving their quantum characteristics [13]. To date, they have been widely used in frequency conversion between quantum systems and telecommunication bands over a span of several hundred terahertz [14–19]. Also, there are attempts to exploit them as interfaces to quantum memory in terms of both the wavelength and waveform [20]. On the other hand, precise frequency transfer

can also be realized with single sideband modulators [21]. But the span of frequency transfer, limited by the bandwidth of rf modulation response, is only tens of gigahertz. Realizing frequency transfer with a span from several hundred gigahertz to several terahertz is essential for DWDM quantum communication, which is still challenging using the aforementioned methods. Although four-wave mixing (FWM) in dispersion-engineered highly nonlinear fiber has been proposed to solve this problem [22], the quantum characteristics preservation feature has not been demonstrated.

In this paper, we report single-photon frequency conversion in a wide telecommunication band based on cascaded quadratic nonlinearity, i.e., SFG and DFG, in a periodically poled lithium niobate (PPLN) waveguide. Although SFG and DFG have been exploited individually in quantum frequency conversion, the cascaded process has not yet been studied at the single-photon level. In this configuration, we show that the frequency of single photons can be precisely transferred to a different frequency with continuous tunability in a wide telecommunication band and their quantum characteristics are maintained after the frequency conversion.

II. THEORY AND EXPERIMENT

In our scheme, the frequency of single photons ω_s is converted to the target frequency ω_t when pumped by two lasers P1 and P2 at ω_{P1} and ω_{P2} simultaneously. Figure 1 shows an energy-level diagram of the SFG and DFG processes as they are coupled via mediate photons (not shown in the figure) with frequency $\omega_m = \omega_s + \omega_{P1} = \omega_t + \omega_{P2}$, according to the energy conservation law. To achieve maximum conversion efficiency, the phase-matching conditions for both the two processes need to be simultaneously satisfied and the two pump lasers are strong without depletion. Then, the quantum physics of this process can be described by the following effective
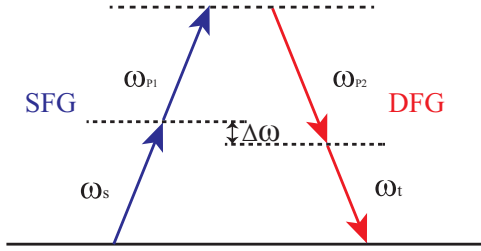
FIG. 1. Level scheme for the cascaded SFG and DFG process. The signal photon (ω_s) is converted to the targeted photon (ω_t) at a lower frequency at the presence of pump1 (ω_{p1}) and pump2 (ω_{p2}) via the SFG and DFG process.

Hamiltonian [13]:

$$\hat{H} = i\hbar(\chi_1 E_{P1}\hat{a}_s\hat{a}_m^\dagger + \chi_2 E_{P2}^*\hat{a}_m\hat{a}_t^\dagger - \text{H.c.}), \qquad (1)$$

where $\hat{a}_i$ is the annihilation operator for the wave at frequency ω_i, with $i = s,m,t$ representing signal, mediate, and target photons, respectively. $\chi_{1,2}$ are coupling constants that are proportional to the second-order susceptibility $\chi^{(2)}$ of the crystal, E_{P1} and E_{P2} are the electric-field amplitudes of pump lasers, and H.c. denotes a Hermitian conjugate. Using the Heisenberg equation of motion, the coupled mode equations describing the cascaded processes can be obtained from Eq. (1):

$$\frac{d\hat{a}_s}{dt} = -\chi_1 E_{P1}^*\hat{a}_m,$$
$$\frac{d\hat{a}_m}{dt} = \chi_1 E_{P1}\hat{a}_s - \chi_2 E_{P2}\hat{a}_t, \qquad (2)$$
$$\frac{d\hat{a}_t}{dt} = \chi_2 E_{P2}^*\hat{a}_m.$$

By applying the boundary conditions $E_{P1}(0) = \sqrt{P_{P1}}\exp(-j\varphi_1)$ and $E_{P2}(0) = \sqrt{P_{P2}}\exp(-j\varphi_2)$ to Eq. (2), the conversion efficiency is yielded as [23]

$$\eta_c(t) = \frac{\langle\hat{a}_t^\dagger(t)\hat{a}_t(t)\rangle}{\langle\hat{a}_s^\dagger(0)\hat{a}_s(0)\rangle} = \frac{\chi_1^2\chi_2^2 P_{P1}P_{P2}|\cos[2(\varphi_1 - \varphi_2)]|}{(\chi_1^2 P_{P1} + \chi_2^2 P_{P2})^2}$$
$$\times \left\{1 - \cos\left[(\chi_1^2 P_{P1} + \chi_2^2 P_{P2})^{(1/2)}t\right]\right\}^2. \qquad (3)$$

Then, after an interaction length of L, the conversion efficiency η_c can be expressed as

$$\eta_c(L) = \frac{\eta_1\eta_2 P_{P1}P_{P2}|\cos[2(\varphi_1 - \varphi_2)]|}{(\eta_1 P_{P1} + \eta_2 P_{P2})^2}$$
$$\times \{1 - \cos[(\eta_1 P_{P1} + \eta_2 P_{P2})^{(1/2)}L]\}^2, \qquad (4)$$

with

$$\eta_1 = \kappa_s\kappa_m\nu^2, \quad \eta_2 = \kappa_{m'}\kappa_t\nu^2, \quad \kappa_i = \left(\frac{2\omega_i^2 n_i d_{\text{eff}}^2}{n_{i1}n_{i2}c\varepsilon_0}\right)^{1/2}, \quad (5)$$

where φ_1 and φ_2 are the phases of the two pumps P1 and P2, respectively. ν is the spatial overlap factor, n_i ($i = m, P1, s, P2, t$) are the crystal refractive indices, and d_{eff} is the effective nonlinear coefficient. c is the vacuum speed of light, and ε_0 is the permittivity of vacuum. η_1 and η_2 are defined as the normalized power efficiencies and $\eta_1 \approx \eta_2 = 1.1/\text{W cm}^2$. Perfect wavelength conversion is achieved when $P_{P1} = P_{P2} = \pi^2/(2\eta_1 L^2)$.

In practice, realizing simultaneous phase matching for two processes is very challenging due to dispersion in a medium. The stringent restriction can be eased using quasi-phase-matching (QPM) schemes. In our experiment, we use a 5-cm-long PPLN waveguide with a poling period of 19.0 μm, to take advantage of both the type-zero QPM configuration and its weak dispersion property in the telecommunication band, which allows simultaneous phase matching for the cascaded SFG and DFG process in a broad bandwidth [24]. Additionally, the cascaded $\chi^{(2)} : \chi^{(2)}$ processes give rise to a large effective third nonlinearity typically 10^4–10^5 times larger than a pure $\chi^{(3)}$ process, which manifests an advantage over its counterpart of FWM, e.g., in fibers [25]. The experimental setup of the frequency convertor is shown in Fig. 2(a). The wavelengths of the two pump lasers P1 and P2 are 1547.72 nm (CH37) and 1544.53 nm (CH41), respectively. Both of them are narrow linewidth cw lasers amplified by erbium doped fiber amplifiers (EDFAs). A set of DWDM filters is used to suppress noise photons by 150 dB. The pump lasers are combined with the signal photons using another set of DWDM filters and then fed to the PPLN waveguide, where the signal photons are converted to the target photons via the cascaded quadratic nonlinearity. At the output of the waveguide, we pick out the target photons with another set of DWDM filters which further suppress the pump lasers by 180 dB. The frequency of the target can be tuned by shifting the wavelength of either pump laser.

To test the performance of the frequency convertor, we use the photon pairs generated from spontaneous parametric down-conversion (SPDC) other than weak coherent pulses. As shown in Fig. 2(b), a 1555.8-nm cw laser amplified by an EDFA is frequency doubled in a PPLN waveguide by second-harmonic generation (SHG). A wavelength division-multiplexing (WDM) filter is used to suppress the 1555.8-nm laser with an extinction ratio of 180 dB. The second harmonic is then used to generate photon pairs through SPDC in another PPLN waveguide. The generated photon pairs are separated from the second harmonic with another WDM with an extinction ratio of about 180 dB. The signal (1554.13 nm, CH29) and idler (1557.36 nm, CH25) photons are then diverted in corresponding DWDM channels using another set of DWDM filters.

The overall conversion efficiency is calculated using the ratio of the net counts of InGaAs single-photon detectors before and after the frequency conversion. In our experiment, the photon-pair generation rate is set to 0.002 per detection gate. Each detection result is accumulated for 1000 s with the dark count subtracted. The measured conversion efficiency is about 0.55% at a low pump power of 20 mW. The noise counts caused by the frequency convertor are about 10^{-7} per detection gate. In principle, perfect conversion can be realized with both pump lasers at 179.5 mW according to Eq. (3). However, only low pump powers are used in our experiment, to avoid damage of the PPLN waveguide. We note that this can be improved by using MgO doped PPLN waveguides which have similar dispersion property but higher damage threshold. Another aspect is that the relative phase between the two pump lasers (P1 and P2) is not locked. Therefore, the random phase difference decreases the conversion efficiency by a factor of 2. Similar to other frequency conversion schemes, eventually the conversion efficiency is limited by the loss of fiber coupling and
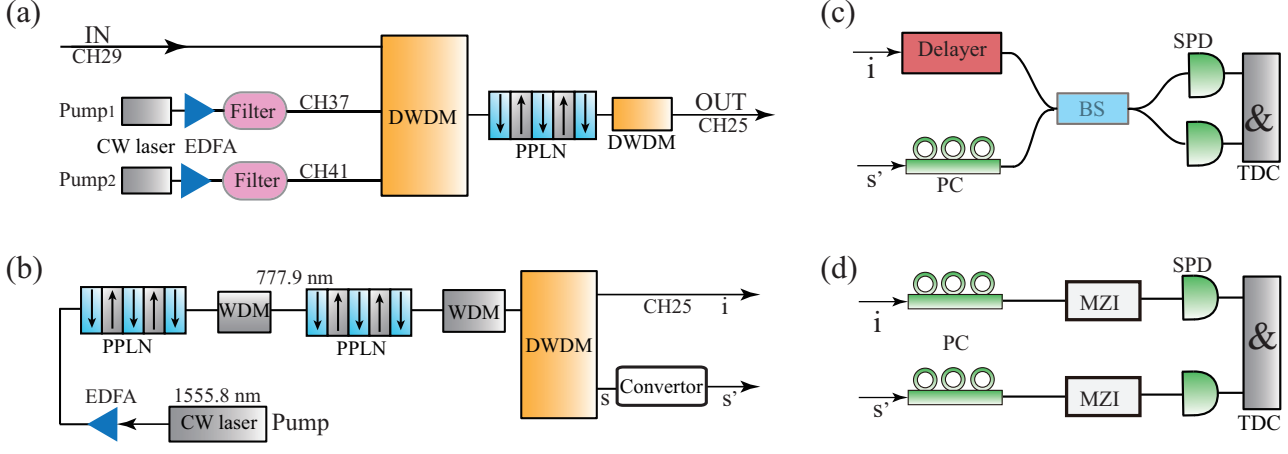
FIG. 2. Experimental setup of (a) the single-photon frequency convertor, (b) photon-pairs preparation, (c) Hong-Ou-Mandel interference, and (d) measurement of time-energy entanglement. EDFA, erbium doped fiber amplifier; WDM, 780–1550-nm wavelength-division multiplexing; DWDM, 100-GHz dense wavelength-division multiplexing; Filter, combination of DWDM and bandpass filter (200–1540 and 1560–1800 nm); CH25 and CH37 and CH41, DWDM channels with 100-GHz spacing defined by ITU-T G.694.1; PC, polarization controller; SPD, single-photon detector (quantum efficiencies, $\eta_d = 10.0 \pm 0.2\%$; repetition frequency of gate, $f = 50$ MHz; width of gate, 1 ns; dark count probability per nanosecond, $D = 1 \times 10^{-6}$); TDC, time-to-digital convertor (coincidence time window, $t = 1$ ns); Delayer, fiber path-length delayer; BS, 50:50 fiber beam splitter; MZI, 1-GHz unbalanced planar lightwave circuit Mach-Zehnder interferometers.

filters, which leaves some room for improvement. For instance, the total loss is about 5.0 dB in Ref. [15] and 7.5 dB in Ref. [18] using DFG in PPLN waveguides, and about 15 dB in Ref. [20] using FWM in fiber. In our experiment, the total propagation and coupling loss in the PPLN waveguide and the filters is only 4.9 dB.

The noises caused by the two pumps are mainly through the cascaded SHG or SFG + SPDC process. Considering that the conversion rate of SPDC is lower than 10^{-6} pairs per pump photon, the numbers of noise photons per second with quasi-phase mismatching (N_{no}) are given by [26]

$$N_{\text{no}} = N_{n1} + N_{n2} + N_{n3}, \quad N_{n1} \approx \xi_1 P_{\text{P1}}^2,$$
$$N_{n2} \approx \xi_2 P_{\text{P2}}^2, \quad N_{n3} \approx \xi_3 P_{\text{P1}} P_{\text{P2}}, \quad (6a)$$

$$\xi_m = \frac{\omega_{s'} \omega_{i'} \omega_{\text{m'}} \omega_{\text{SHm'}} |d_{\text{SH/SF}}|^2 |d_{\text{SP}}|^2}{64 n_{s'} n_{i'} n_{\text{SHm'}}^2 \pi c^6 v^2 \varepsilon_0^2} \Delta \omega$$
$$\times |\Delta \beta_{\text{SH/SF}} \Delta \beta_{\text{SP}}|^{-2}, \quad (6b)$$

where ξ_m ($m = 1, 2, 3$) is the efficiency of SHG or SFG plus SPDC, $d_{\text{SH/SF}}$ and d_{SP} are the effective nonlinear coefficients of SHG or SFG and SPDC, respectively (the effective nonlinear coefficient of SFG is twice that of SHG). $\Delta \omega$ is the 100-GHz bandwidth and $\Delta \beta_{\text{SH/SF/SP}}$ are phase mismatchings of QPM [24]. The measured average photon pair per gate is 8×10^{-4} with 10-mW cw pump with respect to a normalized generation efficiency in CH25. Under this condition, the average noise per gate is 1.76×10^{-7} when the total relative generation efficiency is about 2.21×10^{-4}.

III. RESULTS AND DISCUSSION

In quantum protocols such as quantum teleportation [27] and measurement device independent quantum key distribution [28], it is crucial to realize interference between photons sent by different users. Therefore, in DWDM quantum net-

works, photons in different channels should be converted to the same frequency with high precision. In our experiment, we convert the frequency of the signal photons to that of the idler photons using the frequency convertor and measure the Hong-Ou-Mandel (HOM) interference with the setup shown in Fig. 2(c) [29]. Interference between the idler photons and the frequency shifted signal photons takes place at the 50:50 beam splitter. If the photons are indistinguishable in the two output ports, the two photons will bunch at the same output port. The measured HOM interference, as shown in Fig. 3, shows a clear dip with a fitted visibility of $(80.5 \pm 3.5)\%$, implying the frequency conversion of single photons.

The visibility of the HOM dip is significantly beyond the one that can be obtained with two weak coherent pulses. Besides the noise N_{no} discussed earlier, the degradation of the visibility
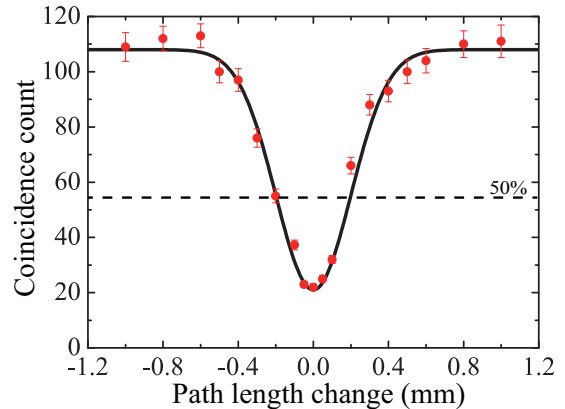

FIG. 3. Coincidence count as a function of the path-length change of one photon. The standard deviation is calculated by assuming a Poisson distribution of photon counts. The dashed horizontal line at 50% is the dividing line between the classical and nonclassical interference.
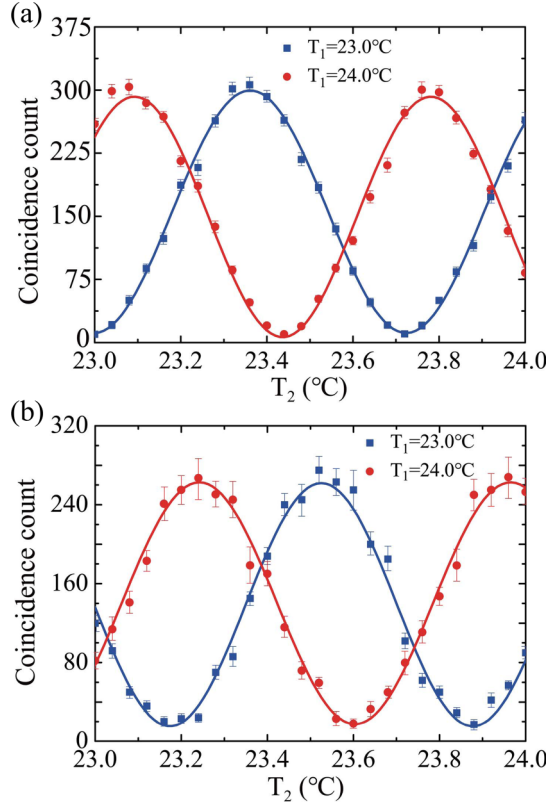
FIG. 4. Two-photon interference pattern (a) before and (b) after the frequency conversion. T_1 is the temperature of the MZI in the signal channel and T_2 is the temperature in the idler channel. The integration time for each dot is (a) 15 s and (b) 3000 s.

is mainly due to the multiphoton-pair emission effect [30] and the dark count of SPDs. In addition, the noises coming from spontaneous Raman scattering may also have some impact on the visibility [31]. In the ideal situation, the visibility of HOM interference after conversion can be expressed as ($\eta_d \ll 1$)

$$V_{\max} = \frac{\eta_c + \eta_c^2 \mu + \eta_c(1 - \eta_c)\mu}{\eta_c + 3\eta_c\mu + 1/2(1 - \eta_c)^2\mu}, \tag{7}$$

where μ is the generation rate of one pair per gate. For $\eta_c = 0.55\%$ and $\mu = 0.2\%$, we find $V_{\max} = 85\%$. The degeneration is mainly caused by the dark count of SPDs.

Another important feature of the frequency convertor is that it maintains the quantum characteristics of signal photons during frequency conversion. To demonstrate this feature, time-energy entanglement between the two signal and idler

photons [32] is measured, which is inherent in photon pairs generated via cw-laser pumped SPDC. The two-photon quantum states generated within the coherence time have a relative phase determined by the product of their time delay τ and the pump laser frequency ($\omega_p = \omega_s + \omega_i$). The time-energy entanglement can be revealed using a Franson-type interferometry as shown in Fig. 2(d). If the relative path delay between the two arms of the interferometer is shorter than the coherence length, interference fringes can be observed by sweeping the relative phase of one interferometer. In our experiment, we use planer lightwave circuit Mach-Zehnder interferometers (MZIs) with 1-ns relative delay. The relative phase is controlled by adjusting the temperature of an MZI device while keeping the other constant. Both the interference fringes before and after the frequency conversion of the signal photons are measured. The measurement results are shown in Fig. 4. We obtain average fitted visibilities of $V = 93.8 \pm 1.6$ and $88.2 \pm 5.1\%$ for time-energy entanglement before and after frequency conversion, respectively. The result convincingly shows that quantum entanglement is well preserved during the frequency conversion. Thus, the photon pairs can still be used for quantum communication tasks. We expect that our scheme may have applications in quantum systems, such as quantum cryptography on multiuser optical fiber networks and quantum teleportation with independent sources.

IV. CONCLUSION

In conclusion, we have demonstrated single-photon frequency conversion using a cascaded quadratic nonlinearity in PPLN waveguides. The clear HOM dip observed in our experiment shows that the frequency has been precisely switched between DWDM channels. Moreover, the time-energy entanglement is well preserved during the frequency conversion. In addition, we note that this quadratic cascading mimics a third-order nonlinearity with an effective $\chi^{(3)}$ much larger than a direct one. Therefore, our scheme has the potential to achieve high efficiency and low noise frequency conversion.

[1] B. Yurke and J. S. Denker, Phys. Rev. A **29**, 1419 (1984).

[2] H. P. Specht, C. Nölleke, A. Reiserer, M. Uphoff, E. Figueroa, S. Ritter, and G. Rempe, Nature (London) **473**, 190 (2011).

[3] M. D. Lukin, M. Fleischhauer, R. Cote, L. M. Duan, D. Jaksch, J. I. Cirac, and P. Zoller, Phys. Rev. Lett. **87**, 037901 (2001).

[4] C. Thiel, T. Böttger, and R. Cone, J. Lumin. **131**, 353 (2011).

[5] A. Imamoglu, D. D. Awschalom, G. Burkard, D. P. DiVincenzo, D. Loss, M. Sherwin, and A. Small, Phys. Rev. Lett. **83**, 4204 (1999).

[6] G. Fuchs, G. Burkard, P. Klimov, and D. Awschalom, Nat. Phys. **7**, 789 (2011).

[7] M. H. Devoret and R. J. Schoelkopf, Science **339**, 1169 (2013).

[8] H.-L. Yin, T.-Y. Chen, Z.-W. Yu, H. Liu, L.-X. You, Y.-H. Zhou, S.-J. Chen, Y. Mao, M.-Q. Huang, W.-J. Zhang *et al.*, Phys. Rev. Lett. **117**, 190501 (2016).

[9] T. Chapuran, P. Toliver, N. Peters, J. Jackel, M. Goodman, R. Runser, S. McNown, N. Dallmann, R. Hughes, K. McCabe *et al.*, New J. Phys. **11**, 105001 (2009).

[10] B. Qi, W. Zhu, L. Qian, and H.-K. Lo, New J. Phys. **12**, 103042 (2010).

[11] H. C. Lim, A. Yoshizawa, H. Tsuchida, and K. Kikuchi, Opt. Fiber Technol. **16**, 225 (2010).

[12] D. Aktas, B. Fedrici, F. Kaiser, T. Lunghi, L. Labonté, and S. Tanzilli, Laser Photon. Rev. **10**, 451 (2016).

[13] P. Kumar, Opt. Lett. **15**, 1476 (1990).

[14] G. Giorgi, P. Mataloni, and F. De Martini, Phys. Rev. Lett. **90**, 027902 (2003).

[15] S. Tanzilli, W. Tittel, M. Halder, O. Alibart, P. Baldi, N. Gisin, and H. Zbinden, Nature (London) **437**, 116 (2005).

[16] K. De Greve, L. Yu, P. L. McMahon, J. S. Pelc, C. M. Natarajan, N. Y. Kim, E. Abe, S. Maier, C. Schneider, M. Kamp *et al.*, Nature (London) **491**, 421 (2012).

[17] S. Zaske, A. Lenhard, C. A. Keßler, J. Kettler, C. Hepp, C. Arend, R. Albrecht, W.-M. Schulz, M. Jetter, P. Michler *et al.*, Phys. Rev. Lett. **109**, 147404 (2012).

[18] P. Manurkar, N. Jain, M. Silver, Y.-P. Huang, C. Langrock, M. M. Fejer, P. Kumar, and G. S. Kanter, Optica **3**, 1300 (2016).

[19] M. Allgaier, V. Ansari, L. Sansoni, C. Eigner, V. Quiring, R. Ricken, G. Harder, B. Brecht, and C. Silberhorn, Nat. Commun. **8**, 14288 (2017).

[20] B. Albrecht, P. Farrera, X. Fernandez-Gonzalvo, M. Cristiani, and H. De Riedmatten, Nat. Commun. **5**, 3376 (2014).

[21] H.-P. Lo and H. Takesue, Optica **4**, 919 (2017).

[22] A. S. Clark, S. Shahnia, M. J. Collins, C. Xiong, and B. J. Eggleton, Opt. Lett. **38**, 947 (2013).

[23] R. V. Roussev, C. Langrock, J. R. Kurz, and M. Fejer, Opt. Lett. **29**, 1518 (2004).

[24] B. Chen and C.-Q. Xu, IEEE J. Quantum Electron. **40**, 256 (2004).

[25] H. Tan, G. Banfi, and A. Tomaselli, Appl. Phys. Lett. **63**, 2472 (1993).

[26] M. Fiorentino, S. M. Spillane, R. G. Beausoleil, T. D. Roberts, P. Battle, and M. W. Munro, Opt. Express **15**, 7479 (2007).

[27] Q.-C. Sun, Y.-L. Mao, S.-J. Chen, W. Zhang, Y.-F. Jiang, Y.-B. Zhang, W.-J. Zhang, S. Miki, T. Yamashita, H. Terai *et al.*, Nat. Photon. **10**, 671 (2016).

[28] H.-K. Lo, M. Curty, and B. Qi, Phys. Rev. Lett. **108**, 130503 (2012).

[29] C.-K. Hong, Z.-Y. Ou, and L. Mandel, Phys. Rev. Lett. **59**, 2044 (1987).

[30] P. Sekatski, N. Sangouard, F. Bussières, C. Clausen, N. Gisin, and H. Zbinden, J. Phys. B **45**, 124016 (2012).

[31] J. S. Pelc, L. Ma, C. Phillips, Q. Zhang, C. Langrock, O. Slattery, X. Tang, and M. Fejer, Opt. Express **19**, 21445 (2011).

[32] J. D. Franson, Phys. Rev. Lett. **62**, 2205 (1989).